Lab on a Chip

Miniaturisation for chemistry, physics, biology, & bioengineering

www.rsc.org/loc

Volume 9 | Number 21 | 7 November 2009 | Pages 3025–3164

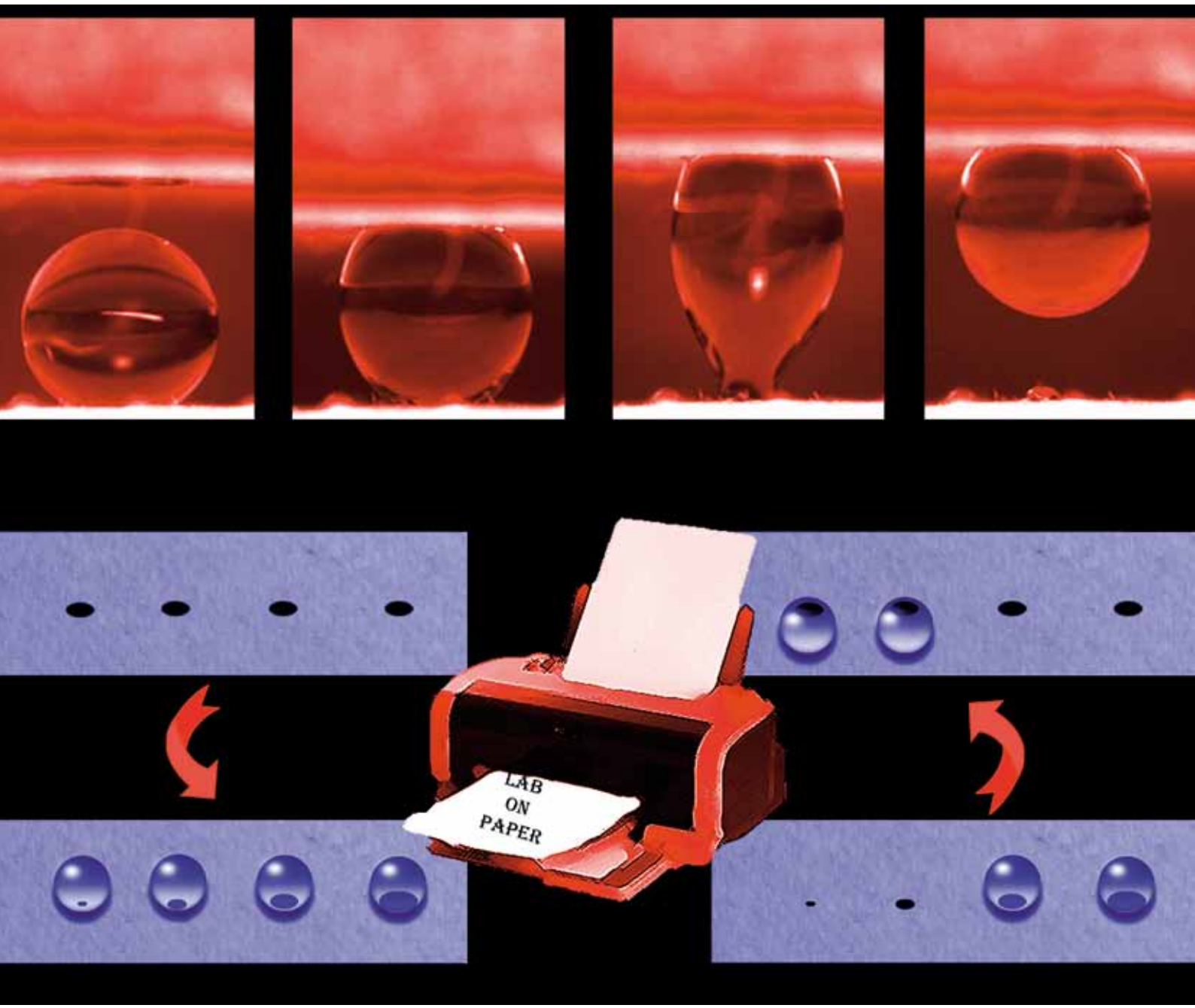

ISSN 1473-0197

RSC Publishing

Patterning of superhydrophobic paper to control the mobility of micro-liter drops for two-dimensional lab-on-paper applications

Balamurali Balu, Adam D. Berry, Dennis W. Hess and Victor Breedveld*

Received 19th May 2009, Accepted 24th July 2009
First published as an Advance Article on the web 5th August 2009
DOI: 10.1039/b909868b

Superhydrophobic paper substrates were patterned with high surface energy black ink using commercially available desktop printing technology. The shape and size of the ink islands were designed to control the adhesion forces on water drops in two directions, parallel ('drag-adhesion') and perpendicular ('extensional-adhesion') to the substrate. Experimental data on the adhesion forces shows good agreement with classical models for 'drag' (Furmidge equation) and 'extensional' adhesion (modified Dupré equation). The tunability of the two adhesion forces was used to implement four basic unit operations for the manipulation of liquid drops on the paper substrates: storage, transfer, mixing and sampling. By combining these basic functionalities it is possible to design simple two-dimensional lab-on-paper (LOP) devices. In our 2D LOP prototype, liquid droplets adhere to the porous substrate, rather than absorbing into the paper; as a result, liquid droplets remain accessible for further quantitative testing and analysis, after performing simple qualitative on-chip testing. In addition, the use of commercially available desktop printers and word processing software to generate ink patterns enable end users to design LOP devices for specific applications.

Introduction

Currently, paper is more than just a substrate for writing, printing and packaging; recent scientific research has established its potential as an inexpensive, biodegradable, renewable, flexible polymer substrate. Innovative concepts of paper-based devices include transistors,[1,2] batteries,[3,4] super-capacitors,[4] MEMS devices,[5] sensors[6] and lab-on-a-chip (LOC) microfluidic devices.[7–14]

We recently reported the fabrication of extremely water repellant superhydrophobic paper surfaces (contact angle (CA) $\sim$166.7 $\pm$ 0.9°; CA hysteresis $\sim$ 3.4 $\pm$ 0.1°) for potential applications in the chemical and biomedical fields *via* plasma treatment.[15–17] In defining superhydrophobicity, researchers often focus on the advancing contact angle, but the receding contact angle plays an important role as well; in a follow-up study we developed protocols to control the adhesion of water drops on paper substrates by tuning the contact angle hysteresis between 149.8 $\pm$ 5.8° and 3.5 $\pm$ 1.1°, while maintaining the advancing CA above 150°.[16] To distinguish between these substrates, we used the terminology "roll-off superhydrophobic" (CA > 150°; hysteresis < 10°) for low hysteresis substrates that exhibit the so-called lotus effect, and "sticky superhydrophobic" for substrates with high hysteresis (CA > 150°; hysteresis > 10°). In this paper, we describe patterning methods that provide local control over droplet adhesion on superhydrophobic paper and use this approach to develop novel paper-based LOC microfluidic devices that enable manipulation (storage, transport, mixing and sampling) of drops of test fluids on the substrate, without absorption of these fluids into the porous paper. These two-dimensional devices can be used for qualitative analytical fluid testing, as well as storage of large arrays of drops for transportation and further quantitative analysis.

In the early stages of their development, LOC microfluidic devices were fabricated with technologies originally developed for the microelectronics industry, in particular photolithography and etching, and thus were fabricated from silicon wafers or glass substrates.[18] Subsequently, researchers began investigating polymers as substrates (especially PDMS) in combination with soft lithography techniques because of the advantages of these substrates over silicon- or glass-based devices: transparency, flexibility, biochemical compatibility and permeability.[18–21] However, even PDMS-based devices require the use of clean room facilities for the fabrication and incorporation of complex components such as valves, pumps and mixers.[18,22–24] Fluid actuation in these devices relies mostly on electrokinetic or pneumatic actuation, which require an external power source (high voltage power supply, batteries, or compressed gas/vacuum sources[25,26]). Overall, in spite of breakthrough advances in LOC concepts, most of the devices remain unsuitable for low-tech applications like biomedical diagnostics in developing countries due to the lack of simplicity and affordability.

Paper-based LOC devices (also referred to as lab-on-paper (LOP)[14]) have emerged as a promising alternative technology. For fluid actuation on these devices one can rely on capillary forces inside the porous paper and thus avoid external power sources. In a recent report on the top ten biotechnologies for improving health in developing countries "modified molecular technologies for affordable, simple diagnosis of infectious diseases" were ranked as the number one priority.[25,27] Another report on the grand challenges for global health ranked the development of technologies to "measure disease and health status accurately and economically in poor countries" first among the top 14 priorities.[25,28] Due to their affordability and

School of Chemical & Biomolecular Engineering, Georgia Institute of Technology, 311 Ferst Drive, Atlanta, GA, 30332-0100, USA. E-mail: victor.breedveld@chbe.gatech.edu; Fax: +1 (404) 894-2866

potentially simple fabrication technology, LOP devices may offer improved global availability of medical technology.

In its simplest form, the concept of LOP dates back to the 1950s, when paper-based strips[29–34] were first used for biomedical diagnostics. However, applications of these LOPs were limited by the fact that they could not perform multiplex analysis: *i.e.*, it was impossible to perform multiple biochemical analyses on a single sample with the same strip. This limitation inspired the fabrication of multiple channels with barriers within a paper substrate, analogous to a microfluidic device, to enable multiplex analysis. Creation of hydrophilic channels with hydrophobic barrier layers for biochemical assay devices was originally proposed in 1995 and 2003.[35,36] More recently, this concept has been adapted by using modern photolithography techniques to create hydrophobic photoresist barriers.[10,11,13] This work has since been expanded to three-dimensional LOP devices by layering sheets of patterned paper with perforated barrier tape to guide the exchange of liquids between paper layers.[12] A disadvantage of these LOPs was the limited flexibility due to the use of rigid photoresists (SU-8 or PMMA), which has been addressed by printing PDMS as a barrier polymer using a desktop plotter, thus creating flexible LOP devices.[8] However, the low surface tension of uncrosslinked PDMS limits the spatial resolution of the patterns, resulting in broad and irregularly shaped barrier wall structures.[8,9] A new two-step method for patterning straight barrier walls was proposed: hydrophobize the entire paper substrate with Alkyl Ketene Dimer (AKD) and then create hydrophilic channels *via* a plasma patterning process.[9] Although both PDMS- and AKD-based LOPs are flexible, the channels are relatively wide (1–2 mm) because of the patterning limitations.[8,9] Controlled fabrication of channels with widths of several hundred micrometers has been achieved by printing hydrophilic patterns *via* inkjet printing.[7] The use of widely available technology to design LOP devices, for example a standard desktop printer, clearly offers substantially enhanced versatility, since it enables end-users to "program" LOP devices according to specific needs. A recent report has noted that programmable LOCs would be the next critical innovation in this technology.[37] Most current LOP technologies limit the ability of non-expert users to program their own devices because of the complex chemicals, methods, and/or equipment needed for device fabrication. Furthermore, all the LOP concepts discussed above depend on absorption of test fluids into the hydrophilic areas of porous paper and use capillary forces for fluid actuation. As a result, the products of reactions occurring inside a LOP cannot easily be extracted for further biochemical analysis. This is particularly important because the analysis in LOPs is currently semi-quantitative at best; the accuracy and sensitivity cannot compete with traditional analytical equipment.[14]

One option to overcome this issue is to prevent absorption of the liquids into the paper matrix. By restricting droplets to the surface of the substrate, the samples are accessible for post-processing and quantitative analysis in a centralized testing center,[25] while simple qualitative biochemical characterizations can still be performed at the point-of-care (POC). In order to achieve this, droplets must be manipulated on a two dimensional substrate that enables basic unit operations: storage, guided transport, mixing and sampling. 2D microfluidic lab-on-chip devices have been previously obtained *via* electrowetting[38,39] and optoelectrowetting (OEW),[40–42] but these approaches require external power sources for operation and complicated fabrication methods. Ideally, a 2D LOP should be inexpensive, enable design flexibility and operate without an external power source.

Our approach, as described below, is to develop a 2D LOP device capable of storage, transfer, mixing and sampling of liquid drops by decorating superhydrophobic paper substrates with high surface energy ink patterns (lines and dots). Surface energy and gravitational forces are used to manipulate and transfer drops, thus eliminating the need for an external power source. The key feature of this device is that patterning changes the local contact angle (CA) hysteresis, resulting in sticky ink spots on non-sticky superhydrophobic paper; the substrates are therefore referred to as Hysteresis Enabled Lab-on-Paper (HELP) substrates. Our study demonstrates that patterns to manipulate microliter drops can be designed using standard word processing software and a commercially available desktop printing process that deposits waxy inks. The simplicity of the soft- and hardware ensures that end-users can readily develop their own patterns to achieve desired functionality of the LOP devices.[37] Finally, the HELP substrates can serve as an inexpensive storage medium for test fluids, reagents and/or reaction products in the form of arrays of drops, which can then be transported to the centralized testing centers for detailed quantitative analysis after initial semi-quantitative on-chip analysis.

This paper demonstrates the fundamental principles behind our LOP concept by measuring and modeling the adhesion of water drops on patterned substrates, and applies this basic knowledge to the design of LOP building blocks with advanced functionality, such as droplet storage, transfer, merger, mixing and sampling.

Experimental details

Superhydrophobic paper

Handsheets were used as model paper substrates and were fabricated following TAPPI-standardized protocol T205 sp-02, using southern hardwood kraft (Alabama River Pulp Co.) and southern softwood kraft (North Carolina International Paper). A more detailed discussion regarding handsheet preparation can be found elsewhere.[15–17] Handsheets were placed inside a 13.56 MHz parallel plate plasma reactor to undergo a two step process (oxygen etching for 60 min to generate roughness and fluorocarbon (pentafluoroethane monomer) film deposition for 1 min to establish surface hydrophobicity) that results in "roll-off" superhydrophobicity as described previously.[15–17]

Patterning

The patterns were designed using standard word processing software (Microsoft® Word 2007). Two types of simple patterns were used: dots and lines. The size of the dots and lines were varied using the font size in "pt"-units, as provided by Microsoft® Word 2007. The "roll-off" superhydrophobic handsheets were pasted on sheets of regular copy paper using Scotch® tape and fed through a Xerox® Phaser 8500n printer to print the patterns designed in the word processing software onto the superhydrophobic handsheet with black phaser ink. Brightfield microscopy images of the printed substrates (Leica microscope

DM4500 B) were used to determine the conversion factor of the patterns from pt-units to μm; images were analyzed using Image J software. For dots, the conversion factor for the dot diameter was found to be 118.5 μm/pt; the conversion factor for line width was 404.9 μm/pt.

Contact angle measurements

Water contact angle measurements were obtained with a Rame–Hart contact angle goniometer (model 100, Netcong, NJ). Advancing and receding contact angles were measured by placing a drop of known volume on the substrate and dragging the paper substrate left to right with respect to the drop; a more detailed description of this method can be found elsewhere.[17,43] In comparison with traditional methods that increase and decrease the drop size at a fixed position, the drag method probes a larger substrate area and yield better statistically averaged CA values, which is particularly important for inherently heterogeneous substrates like paper. Values of the advancing and receding CAs of non-patterned SH paper (after passage through the printer) are $\theta_{ASH} = 165.1 \pm 2^\circ$ and $\theta_{RSH} = 135.3 \pm 2.9^\circ$; for a substrate with full coverage of the ink film, $\theta_{AI} = 113.8 \pm 2.7^\circ$ and $\theta_{RI} = 84.7 \pm 2^\circ$.

Sliding drop experiments

The substrates were mounted on a flat surface attached to a rotating optical stage. The plate was tilted gradually until the drop rolled-off. The angle (in degrees) at which the drop started to slide was defined as the critical sliding angle.

Drop transfer experiments

The drop was placed on a horizontally placed paper substrate which had the "from" pattern (dot). Another substrate having the "to" pattern (line or dot) was then inverted and manually aligned to the drop, to obtain a configuration in which the drop touched the ink patterns on both substrates, which were placed parallel to each other. Then the "to" substrate was carefully lifted in a direction perpendicular to the "from" substrate and the resulting drop dynamics was recorded.

Results and discussion

Adhesion on patterned paper

Sliding drops on sticky islands. In the middle of the 20th century, four research groups independently reported that for a drop sliding on a homogeneous surface, the ratio of the force exerted on the drop (F) to the width of the drop perpendicular to the direction of sliding (W_{drop}) is constant:[44–47]

$$\frac{F}{W_{\text{drop}}} = \frac{\rho V g \sin\alpha}{W_{\text{drop}}} = K_1 \quad (1)$$

where ρ is the density of the liquid drop, V is the volume of the drop, g is the acceleration due to gravity, and α is the critical sliding angle. The constant K_1 was then related to the work functions associated with wetting ($\gamma_{LV}(1 + \cos\theta_A)$) and dewetting ($\gamma_{LV}(1 + \cos\theta_R)$) of the substrate by the drop:[45,46]

$$\frac{\rho V g \sin\alpha}{W_{\text{drop}}} = \gamma_{LV}(\cos\theta_R - \cos\theta_A) \quad (2)$$

where γ_{LV} is the surface tension of the liquid, and θ_A and θ_R are the advancing and receding contact angles of the drop on the surface. This semi-empirical equation, hypothesized by Bikerman[44] in 1950 and derived by Kawasaki[46] in 1960, is popularly known as the Furmidge equation,[45] in reference to the researcher who reiterated it in 1962. This equation is based on a force balance calculation on the receding and advancing edges of a 2D drop sliding on an inclined surface. For a 3D drop, the contact angle varies continuously along the three-phase contact line, which complicates the mathematical analysis. Currently, some disagreement exists in the literature as to whether the local contact angles at the advancing and receding edge of the sliding drop are equal to the experimentally measured maximum (θ_A) and minimum (θ_R) contact angles.[48] In spite of this ambiguity, it has been demonstrated that the Furmidge equation is a good empirical approximation for 3D sliding drops[49] and the Furmidge equation is used by most researchers.[48] After rearranging Eqn 2 we obtain:

$$\frac{V \sin\alpha}{W_{\text{drop}}} = \frac{\gamma_{LV}(\cos\theta_R - \cos\theta_A)}{\rho g} \quad (3)$$

For a specific liquid–surface combination, the right hand side of Eqn 3 is constant. On homogeneous substrates, the volume (V) and width (W_{drop}) of a drop are typically connected *via* simple geometrical relations, so that each drop size corresponds to a unique sliding angle α. In the current work, we aim to disrupt this one-to-one correspondence with the objective to independently control the critical sliding angle (α) and the drop volume (V). Eqn 3 suggests one possible route to achieve this: by making the drop width (W_{drop}) independent of the drop volume (V). In the following paragraphs we will demonstrate how this can be accomplished.

For simplicity, we will assume that the liquid in the following explanation is water. Fig. 1a shows a schematic of the side view of drops with various volumes dispensed on a homogeneous hydrophobic surface (advancing contact angle ~90°). When the drop volume increases, the width of the drop increases as well in

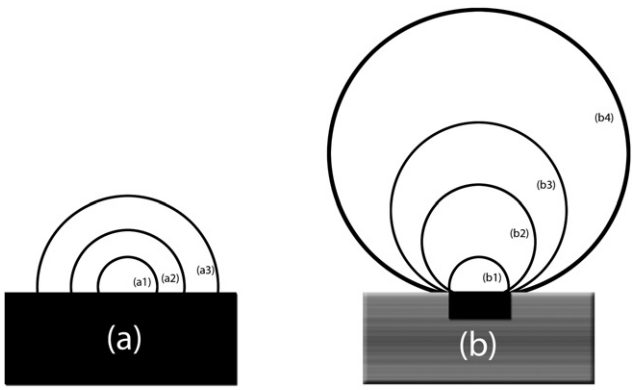

Fig. 1 Schematics of side view profiles for various drop volumes (a) on a homogenous hydrophobic (CA ~ 90°) surface and (b) on a superhydrophobic (CA > 150°) surface with hydrophobic (CA ~ 90°) pattern.

order to maintain a constant contact angle on the substrate. Next, consider the patterned substrate shown in Fig. 1b, where a hydrophobic island (advancing contact angle ~90°, same as in 1a) is surrounded by a superhydrophobic surface (advancing contact angle >150°) which is extremely water repellant. In this case, when more liquid is added to the drop, it does not expand its contact line periphery onto the superhydrophobic substrate until the advancing contact angle of the surrounding superhydrophobic substrate is reached (>150°). As a result, the drop width initially remains constant, while the contact angle changes: the width of the contact area between drop and substrate (W_{drop}) is equal to the size of the sticky island and independent of the volume (V). Only for sufficiently large drops (b4 in Fig. 1b), when the advancing contact angle of the surrounding superhydrophobic substrate is reached, will the base of the drop expand beyond the sticky island. In conclusion, with such patterned substrates, the critical sliding angle (α) at constant drop volume (V) can be manipulated by changing the dimensions of the sticky island (Eqn 3).

We experimentally obtained patterned substrate as follows: "roll-off" superhydrophobicity was first achieved on the paper substrates using plasma etching and deposition.[15–17] The hydrophobic island on the superhydrophobic surface was then obtained by printing "•" (from the symbol menu in Microsoft® Word 2007; designated "dots" in the remainder of this manuscript) using a commercially available phaser printer (Xerox 8500n) and standard black ink. The difference in advancing contact angle between superhydrophobic paper (165.1 ± 2°) and homogeneous full-coverage films of black phaser ink (113.8 ± 2.7°) is sufficient to create the scenario depicted in Fig. 1b. Our superhydrophobic substrate was robust enough that the bending and pressing of the printing process did not affect its advancing CA. Fig. 2 shows the critical sliding angle (angle at which the drop started to slide) *versus* drop volume for different dot sizes

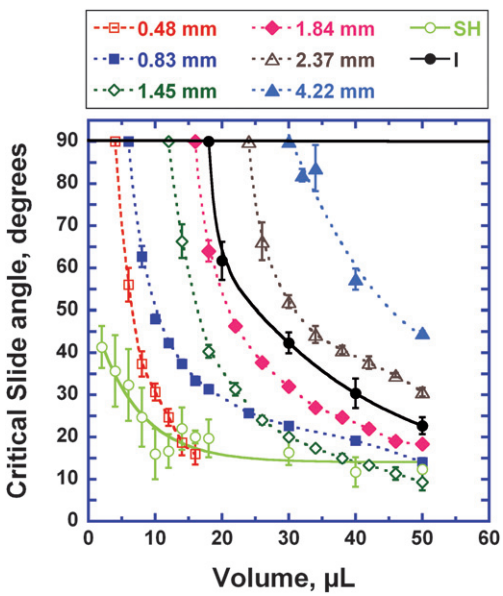

Fig. 2 Critical slide angle *versus* drop volumes on patterned substrates (for various dot sizes) and control substrates (SH and I); curves are to guide the eye.

along with the sliding angles of two homogeneous control substrates (blank superhydrophobic paper after passage through the printer (SH) and a full coverage ink film printed on the superhydrophobic paper surface (I)). Data points on the line that marks the critical slide angle of 90° represent the largest drop that did not slide from vertical substrates. Drop behavior on the control substrates (SH and I) was in good agreement with predictions from a modified Furmidge equation, as will be discussed later in this section. As expected, for each substrate, the critical slide angle decreases monotonically with increasing drop volume (within experimental error). When comparing the results for patterned substrates with the homogeneous control substrates, it is evident from Fig. 2 that at a constant drop volume (V), the critical slide angle (α) increases with increasing dot width. Another interesting observation is that patterned surfaces with large dot sizes (*e.g.*, 2.37 and 4.22 mm) require larger slide angles (*i.e.*, surfaces are more sticky) than a homogenous ink substrate.

Since a continuous ink film essentially is a dot with infinite width, one might have expected that α for the ink film would be higher than for all printed dots. However, this apparent anomaly can be explained using the Furmidge equation. For a drop to slide on a surface, it must deform so that the advancing and receding edge of the drop both reach the experimentally measured advancing and receding CA, respectively, for that substrate. If the drop slides from a printed dot, the advancing CA is set by the superhydrophobic paper, while the receding CA is that of the ink film. In contrast, for homogeneous substrates both advancing and receding contact angles are for the same surface material. For experiments with the smaller dots (<2.37 mm) the initial CA of the drop after dispensing it onto the horizontal substrate was essentially equal to the advancing CA of the superhydrophobic paper surface (similar to configurations b3 or b4 in Fig. 1b), because the drops are large relative to the dot. For the bigger dots, however, the initial CA was closer to the advancing angle on the ink film (configuration b1 in Fig. 1b). Hence, on larger dots a drop must deform to a greater extent before its advancing CA reaches ~ 165.1 ± 2° and the drop starts to slide; thus resulting in higher critical sliding angles for the bigger dots. Fig. 2 demonstrates clearly that the critical sliding angle for drops of any size can be tuned by adjusting the size of the dots printed on the superhydrophobic surface.

The data in Fig. 2 can be interpreted quantitatively by inspecting the Furmidge equation (Eqn 2) more closely. This equation essentially represents a force balance,

$$F_E[= \rho V g \sin\alpha] = F_P[= W_{drop}\gamma_{LV}(\cos\theta_R - \cos\theta_A)] \qquad (4)$$

where F_E is the experimentally measured gravitational force that is necessary to slide a drop on a surface and F_P is the force that can be predicted theoretically from the values of W_{drop}, θ_A and θ_R, which can be determined *via* independent experiments.

Based on Fig. 1b, the width of the drop (W_{drop}) should be equal to the width of the dot (W_{dot}) for a wide range of drop sizes. It was observed experimentally that for large drops, gravity deformed the drops sufficiently to extend the contact line of the drop beyond the dot width (W_{dot}) as shown in Fig. 1b. We denote this as the "outside" configuration (b4) and the corresponding predicted force as F_{PO}. Once the contact line of the drop extends

beyond the ink periphery, the surface energy of the ink film no longer affects the size of the contact area, W_{drop}, or the contact angle θ_A.[50–53] Thus for the F_{PO} configuration, these parameters are determined solely by the properties of the superhydrophobic paper and W_{drop} can therefore be obtained independently by measuring the drop width on non-patterned superhydrophobic paper substrates as a function of drop volume. The results from these experiments (data not shown) were used to calculate W_{drop} for any drops for which $W_{drop} > W_{dot}$. When the substrate in this "outside" drop configuration is tilted, there are two contributions to the adhesion force F_{PO}: one from the part of drop in direct contact with the ink dot (advancing CA of paper substrate (SH) and receding CA of ink (I)) and another from the part of the drop only in contact with the superhydrophobic paper (both advancing and receding CA of SH). Assuming that these force contributions are additive, the predicted force F_{PO} can then be modeled as:

$$F_{PO} = [W_{dot}\gamma_{LV}(\cos\theta_{RI} - \cos\theta_{ASH})] + [(W_{drop} - W_{dot})\gamma_{LV}(\cos\theta_{RSH} - \cos\theta_{ASH})] \quad (5)$$

where θ_{ASH} is the advancing CA of SH paper, θ_{RI} and θ_{RSH} are the receding CAs of the ink film and SH paper, respectively.

If, on the other hand, the drop is confined to the perimeter of the dot (configurations b1–3 in Fig. 1b), the force F_{PP} needed to slide the drop depends only on a single length scale, the dot size (W_{dot}). For this configuration, the second term on the right hand side of Eqn 5 disappears ($W_{dot} = W_{drop}$), resulting in:

$$F_{PP} = [W_{dot}\gamma_{LV}(\cos\theta_{RI} - \cos\theta_{ASH})] \quad (6)$$

The scenario for which $W_{drop} < W_{dot}$ was not encountered with the dot sizes and drop volumes in this study. For homogeneous control substrates (I and SH) there is no need to modify the original Furmidge equation (Eqn. 3), provided that the appropriate CA values are used to calculate the adhesion force (F_I for ink film and F_{SH} for SH paper).

Fig. 3a shows a plot of experimentally determined sliding force F_E *versus* predicted values $F_{PO}/F_{PP}/F_I/F_{SH}$ for a range of drop volumes and dot diameters (0.36 to 4.22 mm, or 3 to 36 pt) including the data presented in Fig. 2. It is evident that the data correspond quantitatively to the predictions from the modified Furmidge equation, which is based on simple geometrical arguments and has no adjustable parameters. Our sliding angle measurements were performed manually, so that slight vibrations induced during the measurements could not be avoided. Also, the SH paper and ink film are both heterogeneous with respect to topography. We believe that the deviations from the model in Fig. 3a for some substrates are a result of these inevitable experimental errors.

We subsequently extended our experiments to a significantly more complicated ink pattern: lines. For these tests, lines were generated using Microsoft® Word 2007 and printed on superhydrophobic paper. We investigated the sliding behavior of drops along the printed lines for different line widths (0.10 to 2.83 mm or 0.25 to 7 pt). It must be noted that the motion of drops on line patterns is anisotropic (parallel *vs* perpendicular to the line). Our initial experiments focused entirely on drop sliding parallel to the lines. In this case, the Furmidge model for the

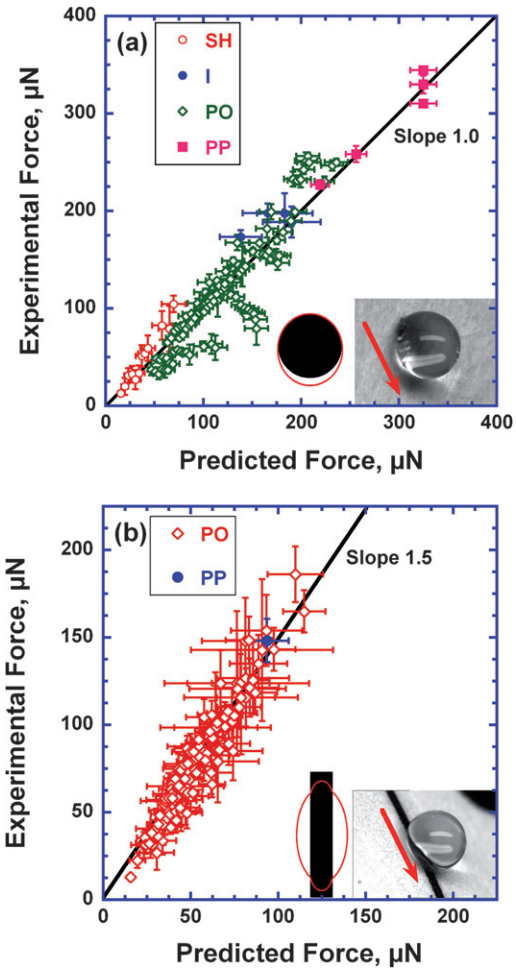

Fig. 3 Experimental *vs* predicted drag-adhesion force for dots (a) and Lines (b) for the following substrates: Superhydrophobic paper after printing a blank pattern (SH), ink film on a SH paper (I), configuration in which the contact line of the drop is outside the ink pattern's periphery (PO) and configuration in which the contact line of the drop is on the ink pattern's periphery (PP). (Insets: Schematic of contact line profile compared to the pattern geometry and photograph of a 4 μL drop just before sliding on a 0.83 mm dot (a) and a 0.3 mm line (b)).

adhesion force for drops that extend outside the line (F_{PO}) can be expressed as

$$F_{PO} = [W_{Line}\gamma_{LV}(\cos\theta_{RI} - \cos\theta_{AI})] + [(W_{drop} - W_{line})\gamma_{LV}(\cos\theta_{RSH} - \cos\theta_{ASH})] \quad (7)$$

where the only difference between Eqn 5 and 7 is that the advancing CA in the first term of (7) is now the advancing CA of the ink; as the drop slides along the line, the part of the drop that resides on the line always remains in contacts with the ink film. Similar to dots, if the drop is contained within the line, $W_{drop} = W_{Line}$ and the second term of the equation vanishes so that

$$F_{PP} = [W_{Line}\gamma_{LV}(\cos\theta_{RI} - \cos\theta_{AI})] \quad (8)$$

Fig. 3b plots experimental sliding force *versus* predicted force (F_{PO} and F_{PP}) for the line patterns. Although a quantitative correlation between model and experiments is obvious, one-to-one

correspondence was not observed. The experimental forces always exceeded the model prediction and linear least-square regression yielded a simple correction factor of 1.5, as indicated by the line in Fig. 3b. Although we have no quantitative explanation for this correction factor, the inset of Fig. 3b clearly shows its qualitative origin: the complicated geometry of the contact line of a drop on a line. The fact that the correction factor is larger than unity can be interpreted as an enhancement of the length of the contact line, which can be attributed to the curvature of the contact line induced by the printed line (see inset in Fig. 3b).

Transfer of drops between substrates. The experiments and models in the previous section give excellent insight into the 'drag adhesion' of drops sliding on substrates patterned with ink dots and lines. This section focuses on the force of adhesion that is observed when drops are pulled-off perpendicular to the patterned substrates. We refer to this kind of adhesion as 'extensional adhesion'. The objective of these experiments was to capitalize on differences in extensional adhesion between different patterned substrates to permit transfer of drops between substrates.

In 1896, Dupré rearranged Young's classical contact angle equation to describe the work of adhesion for a drop to detach from a surface:[54,55]

$$W_{\mathrm{adh}} = \gamma_{LV}(1 + \cos\theta) \tag{9}$$

where θ is the equilibrium CA of the liquid drop on the surface. At that time, the scientific community did not define maximum (advancing) and minimum (receding) CAs.[17,43] When a drop detaches from a surface in a direction perpendicular to the plane of the surface, the contact line of the drop experiences a receding CA value rather than the equilibrium CA.[56] As a result, the above equation must be adapted to

$$W_{\mathrm{adh}} = \gamma_{LV}(1 + \cos\theta_R) \tag{10}$$

This work of adhesion can be converted to the force of adhesion by multiplying the right hand side of the equation by a characteristic length scale, L_{char}:

$$F = L_{\mathrm{char}}\ \gamma_{LV}(1 + \cos\theta_R) \tag{11}$$

For our experiments, it is reasonable to assume that this length scale is proportional to the characteristic size of the ink pattern (dot diameter or line width). Hence, Eqn 11 becomes:

$$F = (\alpha W)\gamma_{LV}(1 + \cos\theta_{RI}) \tag{12}$$

Where α is the proportionally constant and W is the width of the ink pattern. Therefore, it is expected that a drop positioned on a small ink island will experience a smaller force of adhesion than the same drop sitting on a relatively large ink island. This inspired us to determine whether this difference in adhesion force can be used to overcome gravity and transfer a drop from a substrate with a smaller ink island to a substrate with a larger ink island. The resulting force balance between gravity on the drop and adhesive forces of the two substrates is:

$$\rho V g = \alpha_1 W_1 \gamma_{LV}(1 + \cos\theta_{RI}) - \alpha_2 W_2 \gamma_{LV}(1 + \cos\theta_{RI}) \tag{13}$$

where the subscripts 1 and 2 denote the large and small ink islands, respectively. By rearranging the above equation, one can predict the maximum volume of the drop that can be transferred between two substrates:

$$V_{\mathrm{predicted}} = \frac{\alpha_1 W_1 \gamma_{LV}(1 + \cos\theta_{RI}) - \alpha_2 W_2 \gamma_{LV}(1 + \cos\theta_{RI})}{\rho g} \tag{14}$$

We tested the model prediction by determining the *maximum* drop volume that could be transferred (lifted) for a wide variety of dot–dot size combinations. Fig. 4a shows a plot of the experimental *versus* predicted pickup volumes (from Eqn 14) for the various dot–dot configurations used in this study. A linear least-squares regression (data not shown) was performed to find the proportionality constants α_1 and α_2 (in Eqn 14), and the values were found to be $\alpha_1 = \alpha_2 = 1.35$.

A closer look at the force equations for extensional-adhesion (Eqn 12) and drag-adhesion (Eqn 2) reveals that the force needed to overcome extensional-adhesion will always be greater than for drag-adhesion for a specific liquid–substrate combination. This can be explained by comparing Eqn 2 and 12:

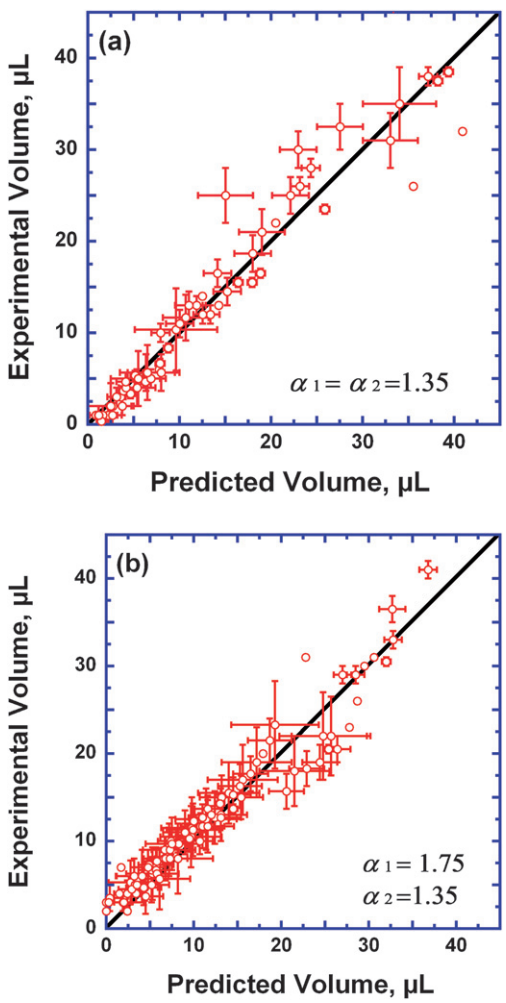

Fig. 4 Experimental *versus* maximum drop pick-up volume for transfer from dot-to-dot (a) and dot-to-line (b); α_1 and α_2 are the fit parameters in Eqn 14.

$$F_{\text{extensional-adhesion}} \sim (1 + \cos\theta_R) > F_{\text{drag-adhesion}} \sim (\cos\theta_R - \cos\theta_A) \quad (15)$$

To achieve equality between the adhesive forces, the advancing CA (θ_A) would have to be 180° which is not possible with our superhydrophobic substrates. Hence, the extensional-adhesion is always greater than the drag-adhesion for our substrates. When the substrates are not parallel to each other during the drop transfer, a combination of drag and extensional adhesion may be experienced and the force balance becomes more complex. The drop transfer experiments were performed manually without using tools to optimize alignment. In spite of this, a good correlation between experimental and predicted values supports our simple model hypothesis.

We further extended our model to the more complex line configurations by determining the transfer of drops from a dot to a line. We selected this configuration (dot-to-line) because of its applicability to the proposed LOP device that is discussed below. In this scenario, the width of the lines and dots were used as the characteristic length scales W_1 and W_2, respectively. The α_2 value of 1.35 was used, as determined from dot–dot transfer experiments. The α_1 value of 1.75 was obtained by linear least-squares regression as discussed previously. Fig. 4b shows the experimental *versus* the predicted pickup volume for the various dot–line configurations used in this report.

In these studies, we have taken advantage of differences in the surface energy between ink and superhydrophobic paper to control the adhesion forces exerted on the drop. Two modes of adhesion exist for the drops, which were designated as 'extensional-adhesion' force and 'drag-adhesion' force, respectively, and these two adhesion forces can be tuned by varying the length scales of the ink patterns.

Functional unit operations with patterned substrates

In the previous section, it was shown that patterned superhydrophobic paper substrates can be used to control the mobility of liquid drops on these substrates, both parallel and perpendicular to the substrate. The underlying mechanism is that the ink patterns locally increase the contact angle hysteresis on a low hysteresis superhydrophobic surface. We therefore refer to these patterned substrates as Hysteresis Enabled Lab-on-Paper (HELP) substrates. In this section, we will discuss how the fundamental wetting properties of these substrates can be used to engineer unit operations that can then be combined in lab-on-paper devices. In the following, we discuss the implementation of four basic functionalities that are critical for any device based on droplet manipulation: storage, transfer, mixing and sampling. The complete list of possible functionalities is certainly longer, especially when more complex ink patterns and modifications in ink chemistry are considered.

Storage. The patterned paper substrates have a peculiar combination of two extreme wetting properties: minimal contact area between liquid and substrate due to high advancing contact angles and good adhesion due to hysteresis. We believe that these properties make HELP substrates potential candidates to serve as storage media for arrays of microliter drops of test fluids and reagents. This type of storage is generally achieved with more expensive well plates that confine liquids in 3D wells with larger interfacial contact areas. We believe that our patterned substrates can provide an inexpensive replacement for current technologies for the storage of array of drops for high throughput screening. The photograph on the left in Fig. 5a shows an array of water drops (colored using food color) stored on a vertical substrate. The three rows had dot sizes of 1.84, 2.37 and 3.32 mm and drops volumes of 15, 20 and 25 μL, respectively. The photograph on the right in Fig. 5a shows a high magnification image of a 12 μL water drop stored on a vertically placed substrate with a 1.7 mm dot. In spite of the low interfacial contact area, the drop withstands a tilt of 90°.

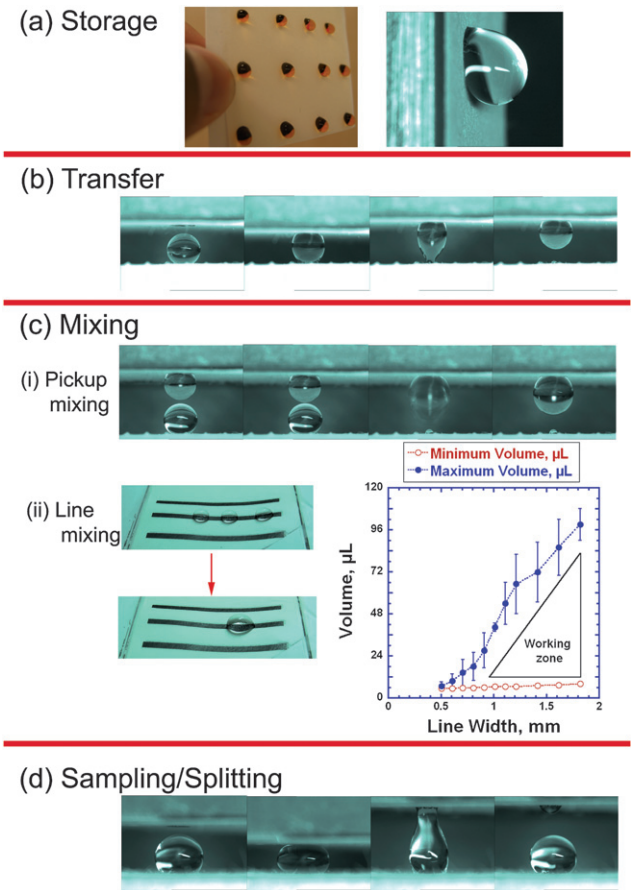

Fig. 5 (a) Photographs of an array of drops (food coloring was added to enhance contrast) and a high magnification image of a single drop stored on a vertical substrate, (b) series of snapshots of a drop being transferred between two substrates, (c) photographs of merging and mixing: (i) *via* "pickup mixing" (two drops), (ii) "line mixing" (three drops) and plot that shows the working zone of drop volumes suitable for line mixing, (d) photographs of drop splitting between two substrates.

Transfer. In a previous section, we investigated the transfer of microliter drops between two patterned substrates with different pattern dimensions and showed that the maximum drop volume that can be transferred between substrates can be predicted using the modified Young–Dupré equation. Fig. 5b shows a sequence of frames from a movie that captured the transfer of a 4 μL water drop from a 0.4 mm dot to a 1.45 mm dot. This functionality enables selective transfer of drops from an array by carefully

tuning the size and location of dots on a pick-up substrate; the superhydrophobicity of the base paper will guarantee that no transfer will occur in non-patterned areas of the pick-up substrate.

Mixing. The patterned paper substrates can also be used to merge and mix liquid drops. We explored two strategies for drop mixing, which we refer to as pickup mixing and line mixing. Fig. 5c (i) shows how two 4 μL water drops (attached to the "from" (0.4 mm) and "to" (1.45 mm) substrates, respectively) are merged into a single drop using pickup mixing. After the two drops are roughly aligned and the substrates are brought together, the drops touch and merge. The final position of the merged drop depends on the competing adhesive forces of the upper "from" and lower "to" dots. As demonstrated previously, the size of "from" and "to" substrates can be tailored to enable pickup mixing for a variety of drop volumes.

The second mixing strategy, line mixing (Fig. 5c (ii)), enables mixing of two or more drops on a line by taking advantage of the fact that the mobility of the drop on the line depends on the drop's configuration on the line. There are three basic configurations that are important for line mixing. (1) If the drop is positioned on the line without touching the end points of the line, the force needed to induce sliding along the line is given by eqn 7 or 8, as discussed previously and shown in Fig. 3b. (2) When a drop slides and reaches the end of the line, its advancing edge contacts the SH paper and hence θ_{AI} in eqn 7 and 8 must be replaced by θ_{ASH}, which results in a significantly increased value of F_{PO} and F_{PP}. Therefore, the sliding angle for a drop at the end of a line is always greater than at other positions. (3) The mobility of a drop perpendicular to the line is much lower than along the line for the same reasons, which restricts drop movement to the line. These considerations concerning drop mobility on a line can be used to design a mixing strategy for drops positioned on the line, by simply tilting the line back and forth drops can be moved towards the line edge, where they become pinned, so that trailing drops can merge. Subsequent rocking of the substrate then moves the merged drop back and forth along the line, which induces internal mixing of the drop. Fig. 5c (ii) shows pictures of the merging and mixing of three 20 μL drops into a single 60 μL drop *via* this line mixing strategy.

There are some limitations to this type of mixing. When drops start sliding, they initially accelerate along the line; if their momentum becomes too large, the adhesive force at the end of the line may be insufficient to ensure adherence to the line edge. Similarly, vibrations can provide energy for the drop to break away from the line. Both effects will limit the maximum drop size for line mixing, but it is beyond the scope of this work to model these phenomena in detail. Instead, we explored the overall effect by evaluating the reproducibility of drop size limits for line mixing. Three individuals with different levels of experience and skill sets performed line mixing experiments and independently determined the minimum and maximum drop volumes that could be mixed for different line widths. The plot in Fig. 5c (ii) shows the results of these tests; the 'working zone' drawn between the two curves denotes the drop volume range for mixing as a function of line width. It is important to point out that these experiments were performed with lines that were 3 cm long. According to our experience with line mixing, longer lines expand the 'working zone' because of improved operator control over the drop position.

Sampling/splitting. Similar to the transfer of drop between two substrates (shown in Fig. 5b), the patterned substrates can also be used to sample small volumes of liquid from a single drop. Fig. 5d shows the sampling of a small volume of liquid to a 1.45 mm dot from an 8 μL drop resting on another 1.45 mm dot. By using closely matched "from" and "to" dot sizes, patterned SH substrates can be used to collect small sample volumes of liquid from a single drop. This functionality is useful in LOP applications in which it is desirable to obtain multiple samples from individual drops for multiplex analysis.

Integrated lab on paper concepts based on HELP substrates

By using the functionalities described in the previous section, it is possible to confine microliter drops to specific locations on a storage substrate, selectively transfer (pick up) drops between substrates, combine/mix drops and sample/split the products into multiple drops. These unit operations can be combined to create a simple lab-on-paper (LOP) device. Fig. 6 shows a schematic of such a LOP device that can be fabricated using the HELP substrates. As starting point, an array of drops is positioned on a substrate using a pattern of dots. In step 1, selected drops are transferred to another substrate which has larger dots printed at specific locations. In step 2, these selected drops are picked up by a third substrate with a line pattern. Finally, in step 3, the three drops on the line are merged into a single drop and mixed *via* 'line mixing'. Thus, selected reactants can be picked up from an array of reactants and mixed to obtain the final product. We would like to emphasize that this specific LOP configuration is just an example of the possible configurations that can be fabricated. The versatility of the printing technique provides the opportunity

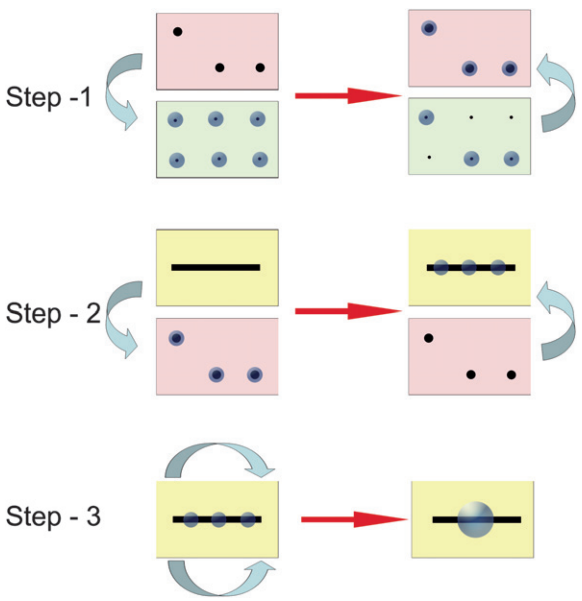

Fig. 6 Schematic of a simple LOP that can be fabricated using the HELP substrates.

to design and create new LOP configurations at the end-user level.

Conclusions

In conclusion, we have made use of commercially available phaser printing technology to pattern superhydrophobic paper substrates with high-hysteresis ink patterns (dots and lines). By tuning the shape and size of the ink patterns, the drag-adhesion and extensional-adhesion of liquid drops to the substrate can be controlled. Experimental results for the adhesive forces of water drops on these patterned substrates are in good agreement with classical models for drag-adhesion (Furmidge equation) and extensional-adhesion (modified Dupré equation) over a wide range of pattern sizes and drop volumes. The fundamental knowledge of the dependence of adhesive forces on pattern parameters and the resulting control over drop mobility were then used to design substrates for four basic functionalities that are relevant for lab-on-paper (LOP) applications: drop storage, drop transfer, drop mixing and sampling.

Previous LOP devices depended on the capillary forces inside the paper to enable the transfer and mixing of test fluids. Hence, this approach rules out the possibility to extract multiple samples of the reaction products for various analyses. In our substrates, we obtain the required unit operations by merely manipulating the liquid drops on top of the substrate by tuning adhesive forces. Another unique advantage of the HELP substrates over existing LOP devices is the ability to store liquid drops after initial, qualitative on-chip analysis for further testing with specialized methods at centralized testing centers, which would be relevant for bioanalytical applications in resource-limited settings.[18] The substrates can also be used as a disposable storage medium in conjunction with high-throughput screening and potentially replace well plate technology.

Finally, the simplicity of the patterning techniques using commercially available desk top printing technology and standard word processing software provides extreme flexibility in substrate design. End-users can easily program their own substrates according to specific needs, using the design rules presented in this paper, which represents the first step towards creating successful LOP devices. Further success of this technology can be achieved by developing custom printing ink formulations to enhance compatibility with various test fluids and facilitate deposition of reagent species.

Acknowledgements

The authors thank Dr. Ashwini Sinha (Praxair) for generously donating the PFE gas, Josie Giles (Georgia Tech) for the help with patterning the SH substrates, Jennifer Sessoms (Georgia Tech) for performing the line mixing experiments and Yan Liu (Georgia Tech) for support with CA measurements. B. B. thanks the Institute for Paper Science and Technology at Georgia Tech for fellowship support.

References

1 W. Lim, E. A. Douglas, S. H. Kim, D. P. Norton, S. J. Pearton, F. Ren, H. Shen and W. H. Chang, *Appl. Phys. Lett.*, 2009, **94**, 072103.
2 R. Martins, P. Barquinha, L. Pereira, N. Correia, G. Goncalves, I. Ferreira and E. Fortunato, *Appl. Phys. Lett.*, 2008, **93**, 203501.
3 M. Murphy, *Chem. Ind.*, 2005, 10–10.
4 P. Rigby, *Mater. Today*, 2007, **10**, 9–9.
5 J. Kim, S. Yun and Z. Ounaies, *Macromolecules*, 2006, **39**, 4202–4206.
6 D. Nilsson, T. Kugler, P. O. Svensson and M. Berggren, *Sens. Actuators, B*, 2002, **86**, 193–197.
7 K. Abe, K. Suzuki and D. Citterio, *Anal. Chem.*, 2008, **80**, 6928–6934.
8 D. A. Bruzewicz, M. Reches and G. M. Whitesides, *Anal. Chem.*, 2008, **80**, 3387–3392.
9 X. Li, J. F. Tian, T. Nguyen and W. Shen, *Anal. Chem.*, 2008, **80**, 9131–9134.
10 A. W. Martinez, S. T. Phillips, M. J. Butte and G. M. Whitesides, *Angew. Chem., Int. Ed.*, 2007, **46**, 1318–1320.
11 A. W. Martinez, S. T. Phillips, E. Carrilho, S. W. Thomas, H. Sindi and G. M. Whitesides, *Anal. Chem.*, 2008, **80**, 3699–3707.
12 A. W. Martinez, S. T. Phillips and G. M. Whitesides, *Proc. Natl. Acad. Sci. U. S. A.*, 2008, **105**, 19606–19611.
13 A. W. Martinez, S. T. Phillips, B. J. Wiley, M. Gupta and G. M. Whitesides, *Lab Chip*, 2008, **8**, 2146–2150.
14 W. A. Zhao and A. van den Berg, *Lab Chip*, 2008, **8**, 1988–1991.
15 B. Balu, V. Breedveld and D. W. Hess, *Langmuir*, 2008, **24**, 4785–4790.
16 B. Balu, J. S. Kim, V. Breedveld and D. W. Hess, in *Contact Angle Wettability and Adhesion*, ed. K. Mittal, Koninklijke Brill NV, Leiden (Netherlands), 2009.
17 B. Balu, J. S. Kim, V. Breedveld and D. W. Hess, *J. Adhes. Sci. Technol.*, 2009, **23**, 361–380.
18 G. M. Whitesides, *Nature*, 2006, **442**, 368–373.
19 J. M. K. Ng, I. Gitlin, A. D. Stroock and G. M. Whitesides, *Electrophoresis*, 2002, **23**, 3461–3473.
20 G. M. Whitesides and A. D. Stroock, *Phys. Today*, 2001, **54**, 42–48.
21 N. T. Nguyen and Z. G. Wu, *J. Micromech. Microeng.*, 2005, **15**, R1–R16.
22 D. B. Weibel, M. Kruithof, S. Potenta, S. K. Sia, A. Lee and G. M. Whitesides, *Anal. Chem.*, 2005, **77**, 4726–4733.
23 N. T. Nguyen, X. Y. Huang and T. K. Chuan, *J. Fluids Eng.*, 2002, **124**, 384–392.
24 A. Gunther, M. Jhunjhunwala, M. Thalmann, M. A. Schmidt and K. F. Jensen, *Langmuir*, 2005, **21**, 1547–1555.
25 C. D. Chin, V. Linder and S. K. Sia, *Lab Chip*, 2007, **7**, 41–57.
26 S. K. Sia, V. Linder, B. A. Parviz, A. Siegel and G. M. Whitesides, *Angew. Chem., Int. Ed.*, 2004, **43**, 498–502.
27 A. S. Daar, H. Thorsteinsdottir, D. K. Martin, A. C. Smith, S. Nast and P. A. Singer, *Nat. Genet.*, 2002, **32**, 229–232.
28 H. Varmus, R. Klausner, E. Zerhouni, T. Acharya, A. S. Daar and P. A. Singer, *Science*, 2003, **302**, 398–399.
29 J. P. Comer, *Anal. Chem.*, 1956, **28**, 1748–1750.
30 N. Delacruz, K. F. Button and S. R. Gambino, *Am. J. Clin. Pathol.*, 1983, **80**, 118–118.
31 A. Reinhartz, S. Alajem, A. Samson and M. Herzberg, *Gene*, 1993, **136**, 221–226.
32 S. Tsuda, M. Kameyaiwaki, K. Hanada, Y. Kouda, M. Hikata and K. Tomaru, *Plant Dis.*, 1992, **76**, 466–469.
33 H. H. Yeoh, L. S. Lim and H. C. Woo, *Biotechnol. Tech.*, 1996, **10**, 319–322.
34 W. A. Zhao, M. M. Ali, S. D. Aguirre, M. A. Brook and Y. F. Li, *Anal. Chem.*, 2008, **80**, 8431–8437.
35 M. P. Allen, Chemtrak Inc., *US Pat.* 5,409,664, 1995.
36 J. D. Hardman, J. H. Slater, A. G. Reid, W. K. Lang and J. R. Jackson, Diamatrix Limited, *US Pat.* 6,573,108, 2003.
37 S. F. Gale, in *Small Times*, 2009, pp. 18–20.
38 M. Abdelgawad and A. R. Wheeler, *Adv. Mater.*, 2009, **21**, 920–925.
39 A. R. Wheeler, *Science*, 2008, **322**, 539–540.
40 P. Y. Chiou, H. Moon, H. Toshiyoshi, C. J. Kim and M. C. Wu, *Sens. Actuators, A*, 2003, **104**, 222–228.
41 P. Y. Chiou, S. Y. Park and M. C. Wu, *Appl. Phys. Lett.*, 2008, **93**, 221110.
42 H. S. Chuang, A. Kumar and S. T. Wereley, *Appl. Phys. Lett.*, 2008, **93**, 064104.
43 A. M. Gaudin, A. F. Witt and T. G. Decker, *Trans. Soc. Mining Eng. AIME*, 1963, **226**, 107–112.
44 J. J. Bikerman, *J. Colloid Sci.*, 1950, **5**, 349–359.
45 G. C. L. Furmidge, *J. Colloid Interface Sci.*, 1962, **17**, 309–324.
46 K. Kawasaki, *J. Colloid Sci.*, 1960, **15**, 402–407.

47 G. Macdougall and C. Ockrent, *Proc. R. Soc. London, Ser. A*, 1942, **180**, 0151–0173.
48 B. Krasovitski and A. Marmur, *Langmuir*, 2005, **21**, 3881–3885.
49 P. Roura and J. Fort, *Langmuir*, 2002, **18**, 566–569.
50 L. C. Gao and T. J. McCarthy, *Langmuir*, 2007, **23**, 3762–3765.
51 L. C. Gao and T. J. McCarthy, *Langmuir*, 2007, **23**, 13243–13243.
52 G. McHale, *Langmuir*, 2007, **23**, 8200–8205.
53 M. V. Panchagnula and S. Vedantam, *Langmuir*, 2007, **23**, 13242–13242.
54 E. D. Hondros, *J. Mater. Sci.*, 2005, **40**, 2119–2123.
55 S. Wu, *Polymer Interface and Adhesion*, Marcel Dekker, Inc., New York, 1982.
56 E. J. De Souza, L. Gao, T. J. McCarthy, E. Arzt and A. J. Crosby, *Langmuir*, 2008, **24**, 1391–1396.